Reentrant Melting in Laser Field Modulated Colloidal Suspensions

J. Chakrabarti,[1] H. R. Krishnamurthy,[1,*] A. K. Sood,[1,*] and S. Sengupta[2]

[1]*Department of Physics, Indian Institute of Science, Bangalore 560 012, India*

[2]*Materials Science Division, Indira Gandhi Centre for Atomic Research, Kalpakkam 603 102, India*

(Received 17 April 1995)

We present results from a Monte Carlo simulation study of the phase diagram and the order of the modulated liquid to crystal transition in laser field modulated colloids. We find that for low values of βV_e, the strength of the modulation potential, the transition is first order, but changes to a continuous transition for high values of βV_e, in agreement with the conclusions from the density functional theory of laser induced freezing. However, we find in the simulation a novel reentrant laser induced melting transition from the crystal to the modulated liquid phase with increasing βV_e, unlike the (mean field) density functional phase diagram.

PACS numbers: 82.70.Dd, 64.70.Dv

In this Letter we present results from our recent Monte Carlo (MC) simulation studies of laser field modulated colloids which show a *novel reentrant laser induced melting* transition from the crystalline to modulated liquid phase.

Studies of laser field modulated colloids date back to the pioneering work of Chowdhury, Ackerson, and Clark [1], who demonstrated *laser induced freezing* (LIF) in a two-dimensional (2D) suspension of strongly interacting colloidal particles. They showed that the colloidal liquid freezes into a 2D crystal with predominantly hexagonal order, when subjected to a 1D modulation potential V_e (induced by a standing wave pattern of interfering laser beams) with its wave vector q tuned to q_0, the first peak of the direct correlation function (DCF) $c^{(2)}(q)$ of the colloidal liquid. Chowdhury, Ackerson, and Clark [1] also theoretically analyzed this phenomenon in terms of a simple Landau-Alexander-McTague [2] theory and concluded that the transition from the 1D modulated liquid to the 2D (modulated) crystalline phase can be made continuous for sufficiently large V_e. Later studies of these phenomena involving direct microscopic observations [3] as well as MC simulations [4] confirmed the existence of LIF, but their conclusions regarding the nature of the transition between the modulated liquid and the crystal were not definitive.

The question of the order of the LIF transition has been studied recently using density functional theory (DFT) [5,6]. In Ref. [6] it has been shown how the *modulated liquid* $\rightarrow$ *crystal* transition can change from first order to a continuous one via a tricritical point with increasing V_e. When the modulation wave vector is tuned to q_0, V_e couples to the density (order parameter) modes of the crystal belonging to a subset $\{\vec{g}^{(f)}\}$ of the set of smallest reciprocal lattice vectors (RLV's), $\{\vec{g}^{(o)}\}$. Symmetry considerations indicate that the order parameters corresponding to $\{\vec{g}^{(o)}\}$ can then be divided into two classes: (1) those corresponding to $\{\vec{g}^{(f)}\}$, the modulation wave vectors, with a value we denote by ξ_f; and (2) those corresponding to the rest, $\{\vec{g}^{(d)}\}$ [$\equiv \{\vec{g}^{(0)}\} - \{\vec{g}^{(f)}\}$], which we denote by ξ_d. The key point is that one can choose $\{\vec{g}^{(f)}\}$ in such a way that an integral combination of vectors in $\{\vec{g}^{(f)}\}$ cannot be obtained from an odd combination of vectors in $\{\vec{g}^{(d)}\}$ [6]. Under this condition [6] the Landau free energy expansion about the modulated liquid phase (with $\xi_f \neq 0$) in powers of ξ_d has only even powers and the transition changes from first order for low values of βV_e (where the quartic coefficient of the Landau free energy is negative) to a continuous one for large values of βV_e (where the quartic coefficient is positive) via a tricritical point [$\beta \equiv (k_B T)^{-1}$].

In the light of this work, careful and extensive simulation studies of such systems to investigate the phase diagram and the nature of the transition are of obvious interest, especially because the earlier MC simulations did not focus on these issues. In this Letter we report the results of such studies on a 2D polyball system (diameter, $2R = 1.07$ μm) of concentration $n_p = 1.81 \times 10^7/\text{cm}^2$, subjected to an external potential of the form $U(\vec{r}) = -V_e \cos(q_0 x)$ with $q_0 = 2\pi/(\frac{\sqrt{3}}{2} a_s)$ [where $a_s \equiv (\frac{\sqrt{3}}{2} n_p)^{-1/2}$ is the interparticle separation], the smallest RLV of the crystalline phase, or equivalently the position of the first peak of the liquid DCF. This choice, leading to $\{\vec{g}^{(f)}\} = \frac{2\pi}{a_s\sqrt{3/2}}(\pm 1, 0)$ and $\{\vec{g}^{(d)}\} = \frac{2\pi}{a_s\sqrt{3/2}}(\pm\frac{1}{2}, \pm\frac{\sqrt{3}}{2})$, satisfies the symmetry condition stated above [6]. The interaction between two polyballs separated by a distance r is taken to be of the standard DLVO (after Derjaguin, Landau, Verwey, and Overbeek) form [7]

$$V(r) = \frac{(Z^* e)^2}{\epsilon}\left(\frac{\exp(\kappa R)}{1 + \kappa R}\right)^2 \frac{\exp(-\kappa r)}{r}.$$

Here $Z^* e$ ($Z^* = 7800$ as in [4]) is the effective surface charge, ϵ ($= 78$) is the effective dielectric constant of the solvent, and κ is the inverse of the Debye screening length due to the counterions in the solvent [8]. The order of the transition is analyzed using the finite size scaling

 0031-9007/95/75(11)/2232(4)$06.00

behavior of $A_L \equiv [\langle E^4\rangle/(3\langle E^2\rangle^2) - 1/3]$ (where E is the total potential energy of the system). It has been shown [9] that A_L shows distinctive finite size dependences depending on the nature of the transition. In the case of a first-order transition (see Ref. [9] for details), A_L shows a dip ($A_L^{\min}$) at a temperature $T_0^{\min}$ such that as $L \to \infty$ $T_0^{\min}$ tends to T_0, the phase coexistence point, and $A_L^{\min}$ tends to a nontrivial value different from zero, with a finite size correction varying as L^{-d} where d is the spatial dimensionality:

$$A_L^{\min} = \frac{1}{3}\frac{(E_+^2 - E_-^2)^2}{(2E_+E_-)^2} + O(k_B T_0^2 L^{-d}). \quad (1)$$

Here E_+ and E_- are the energies of the ordered and the disordered phases, respectively. In the case of a continuous transition, on the other hand, from finite size scaling one can show [9] that $A_L^{\min}$ goes to zero as $L^{-(d-\alpha/\nu)}$ as $L \to \infty$. Hence by looking at the L dependence and the limiting (i.e., extrapolated) values of A_L, one is able to distinguish first-order and continuous transitions even from finite sized MC simulations.

Our simulations were carried out on $N = L^2$ particles in a rectangular box with $L_x/\frac{\sqrt{3}}{2} = L_y = La_s$ so that the formation of the hexagonal lattice (to which the system is known to freeze when $V_e = 0$) does not get frustrated. Periodic boundary conditions (PBC's) were used in both the directions. We fixed βV_e at a given value and scanned along the κa_s axis. For each κa_s, the simulations were carried out for different system sizes ($L = 2n$, $n =$ 3, 4, 5, 6, and 10). The starting configuration was a triangular lattice with slight perturbation at each lattice point. The configurations were then updated by means of a standard Metropolis algorithm [10]. The cutoff of the interaction potential was kept at the distance where the DLVO potential falls to $0.001k_BT$. The energy of interaction was computed using the minimum image convention and the computation was speeded up by constructing a Verlet neighbor list updated at regular intervals (the interval depends on the point in the phase diagram where the simulation is being carried out). The size of the MC step was so chosen that the acceptance ratio [10] was ~0.40. We studied extensively the limiting case $V_e = \infty$ whence the MC moves in the transverse (x) direction are not allowed. This particular limit is of interest because according to DFT [6] the transition from the modulated liquid to solid must be continuous for very large V_e. The equilibration was judged by monitoring $\langle E\rangle$, A_L, and the specific heat C_V [11]. After equilibration, typically 10000 MC steps were carried out for calculating average of interest. For $\beta V_e =$ 0 and $\beta V_e = \infty$ we present, in addition to the bulk equilibrium quantities like $\langle E\rangle$, A_L, and C_V, preliminary results for the Fourier components of density $\rho(\vec{q})$ using the definition $\rho(\vec{q}) = \langle \Sigma_i^N e^{i\vec{q}\cdot\vec{r}_i}\rangle$. Here $\langle\,\rangle$ indicates configuration averaging, $\vec{q} = (2\pi n_x/L_x, 2\pi n_y/L_y)$, n_x and n_y being integers, as allowed by the PBC, and the particle coordinates are measured in the center of mass frame to take care of the center of mass drift during the simulation. Note that $\vec{q} = \{\vec{g}^{(d)}\}$ corresponds to $n_x = \pm n$ and $n_y = \pm 2n$. We have computed $\rho(\vec{q})$ only for those $\vec{q}$ for which the (integral) values of n_x and n_y are close to n and $2n$, respectively. We define the numerical value of the maximum in $\rho(\vec{q})$ as the "order parameter" ρ_m. We have also calculated (for specific cases) the single particle density $\rho(\vec{r})$ by binning the x and y coordinates of the particles (with respect to the center of mass) into a rectangular mesh and averaging over typically 10000 configurations.

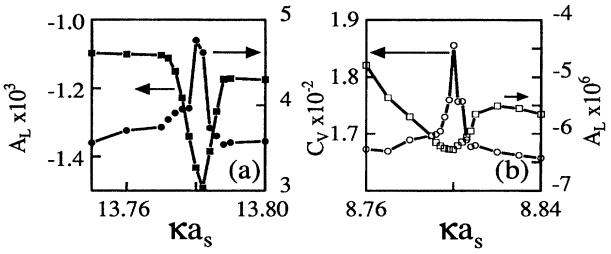

FIG. 1. Plots of A_L and C_V as functions of κa_s for (a) $\beta V_e = 0$ and (b) $\beta V_e = \infty$.

First we discuss our results for the case $\beta V_e = 0$ for which the freezing transition is known to be first order. We find, as shown in Fig. 1(a), that A_L shows a pronounced dip and C_V has a pronounced peak at the same value of κa_s, which we denote by $\kappa_L^* a_s$. We obtain the transition point $\kappa^* a_s$ (= 13.8 for $\beta V_e =$ 0), i.e., by extrapolating the κ_L^* data (which have a weak L^{-1} dependence) to $L \to \infty$. For $\beta V_e = 0$, the energies $E_\pm$ for κa_s slightly larger and smaller than $\kappa_L^* a_s$ for the largest system size ($L = 20$) are different, but the difference is so small that $\lim_{L\to\infty} A_L \simeq 6 \times 10^{-4}$ [cf. Eq. (1)]. Ignoring this small constant, the log-log plot of $A_L^{\min}$ vs L^{-1}, shown in Fig. 2(a), gives a best fitting exponent of 2.05. This we take as an indication that the transition is first order. This conclusion is also supported by our data for the order parameter ρ_m for $L = 10$ and 20 shown in Fig. 3(a), which jump to zero. We find that the jumps in ρ_m happen at κa_s values which are larger than $\kappa_L^* a_s$, and much more strongly L dependent, but extrapolating to the same $\kappa^* a_s$ as $L \to \infty$.

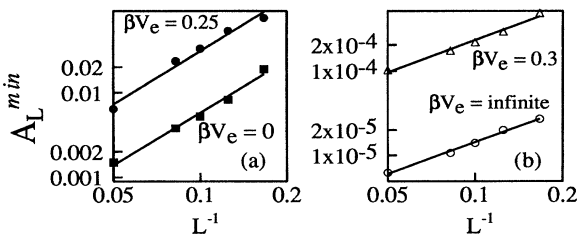

FIG. 2. Log-log plot of $A_L^{\min}$ vs L for different external potentials (a) with lines of slope 2.05 indicating first-order transitions and (b) with lines of slope 1.24 indicating continuous transitions.

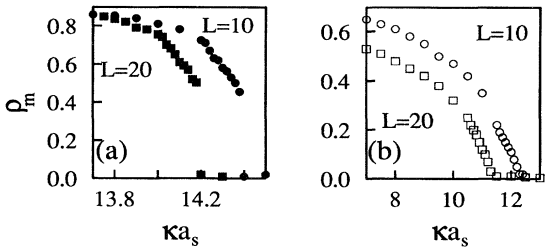

FIG. 3. ρ_m vs κa_s plot for (a) $\beta V_e = 0$ and (b) $V_e = \infty$.

Next we consider the limiting case of $\beta V_e = \infty$. Here also [cf. Fig. 1(b)] A_L shows a pronounced dip and C_V a pronounced peak at $\kappa_L^* a_s$, with $\lim_{L\to\infty} \kappa_L^* a_s \equiv \kappa^* a_s = 8.9$. The log-log plot of $A_L^{\min}$ vs L^{-1} shown in Fig. 2(b) has the best fitting exponent of 1.24. This, together with the negligible limiting value of $A_L^{\min}$ ($\simeq 3 \times 10^{-6}$, as estimated using Eq. (1) from the $E_\pm$ values for this case), we take as evidence that the transition is continuous [12]. In support are the data for the order parameter ρ_m for $L = 10$ and 20 in Fig. 3(b) which vanish continuously, but again at a value of κa_s larger than $\kappa_L^* a_s$, presumably due to a combination of finite size effects and possible critical slowing down near the transition point [13].

We have carried out a similar scaling analysis of $A_L^{\min}$ for $\beta V_e = 0.05$, 0.25, 0.3, and 0.5. The exponent is found to be close to 2 for $\beta V_e = 0.05$ and 0.25 and it is close to 1.26 for $\beta V_e = 0.3$ and 0.5. The values of the exponent indicate that the transition is first order up to $\beta V_e = 0.25$ and continuous from $\beta V_e = 0.3$ onwards with a tricritical point lying in between $\beta V_e = 0.25$ and 0.3. This, together with $\kappa^* a_s$ values we have obtained for other finite values of βV_e up to $\beta V_e = 1$, gives us the phase diagram shown in Fig. 4. It is clear from Fig. 4 that for low values of βV_e (up to $\beta V_e = 0.2$) the transition takes place at higher κa_s [lower $(\kappa^* a_s)^{-1}$] with increasing βV_e. This is clearly the phenomenon of LIF. For high values of βV_e, however, the transition point bends back to lower values of κa_s

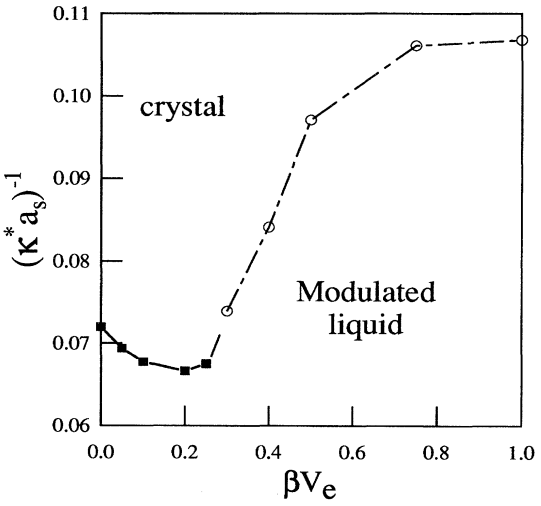

FIG. 4. The phase diagram in the $[(\kappa^* a_s)^{-1}, \beta V_e]$ plane. Filled squares denote first-order transition points and the open circles denote the continuous transition points.

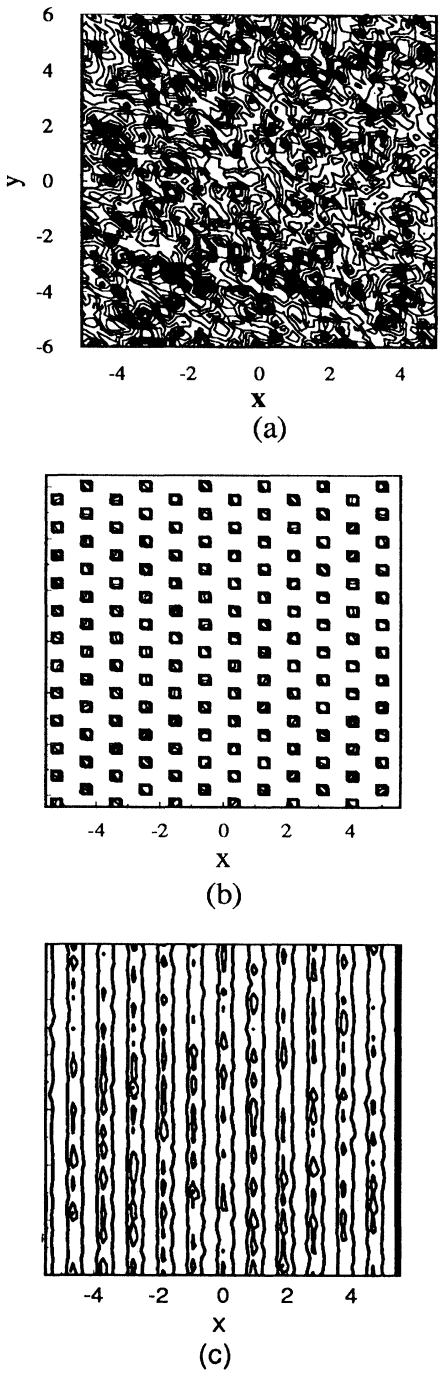

FIG. 5. Contour plots of $\rho(\vec{r})$ for $(\kappa^* a_s)^{-1} = 0.7$ indicating (a) liquid ($\beta V_e = 0$), (b) crystal ($\beta V_e = 0.2$), and (c) modulated liquid ($\beta V_e = 0.5$) phases.

[higher $(\kappa^* a_s)^{-1}$], i.e., to larger interaction strength, with increasing βV_e, eventually saturating around $(\kappa^* a_s)^{-1} = 0.11$ (for $\beta V_e = \infty, (\kappa^* a_s)^{-1} = 0.112$). This saturation implies that for points very deep into the crystal region [for $(\kappa^* a_s)^{-1} \geq 0.11$], one will always get a stable crystalline phase, no matter how large βV_e is. This feature is in agreement with the DFT and contrasts with the behavior found in the Landau-type theories [6].

However, there are two novel aspects of the phase diagram in Fig. 4 that did not show up in the DFT analysis of Ref. [6]. First, for $(\kappa^* a_s)^{-1} \geq 0.072$, as βV_e increases, one will get *a laser induced melting (LIM) transition*. Second, for $0.066 < (\kappa^* a_s)^{-1} < 0.072$, LIF is followed by a *LIM transition to a reentrant modulated liquid phase* with increasing βV_e. Our results for the single particle density $\rho(\vec{r})$ along the line $(\kappa^* a_s)^{-1} = 0.07$ for $\beta V_e = 0.0$, 0.2, and 0.5 on a 12×12 lattice shown in Figs. 5(a)–5(c), indicate that for $\beta V_e = 0$, the phase is liquid, for $\beta V_e = 0.2$, it is a triangular lattice, and for $\beta V_e = 0.5$ a modulated liquid phase, clearly supporting reentrant phase transition.

In summary, our simulation studies are in agreement with the conclusions of the DFT that the transition from the modulated liquid phase to the crystal changes from first order to *continuous* with increasing values of βV_e via a *tricritical point.* However, in contrast to the findings in the DFT, novel features, namely, a *LIM transition* and a *reentrant modulated liquid* phase are seen in the phase diagram [14]. It is clearly of great interest to understand the physical mechanisms behind these features. Likely to be important are fluctuation effects beyond the mean field theory of Ref. [6]; for, apart from the fluctuation effects due to the fact that our system is 2D, as βV_e increases, the particle motion in directions transverse to the modulation is restricted, leading to reduced effective dimensionality and enhanced fluctuations [15]. In addition, the changes in the liquid structure factor due to V_e have not been taken into account in the theory of Ref. [6], and may also be important in high βV_e region. These are also the likely reasons why the location of the tricritical point in Fig. 4 (βV_e between 0.25 and 0.30) differs substantially from the density functional prediction [6] ($\beta V_e \simeq 0.1$). Our results clearly indicate that new experimental studies of laser field modulated colloids look for the continuous modulated liquid to crystal transition as well as LIM and the reentrant liquid phase, and further theoretical studies would be of great interest.

We thank the Indo-French Centre for the Promotion of Advanced Research and the Council for Scientific and Industrial Research for financial support; the Supercomputer Education and Research Centre at the Indian Institute of Science for computing facilities; Siddhartha Shankar Ghosh, Sriram Ramaswamy, T.V. Ramakrishnan, and Madan Rao for discussions; and Chinmay Das for help with the preparation of the paper.

*Also at Jawaharlal Nehru Center for Advanced Scientific Research, IISc Campus, Bangalore 560 012 India.

[1] A. Chowdhury, B.J. Ackerson, and N.A. Clark, Phys. Rev. Lett. **55**, 833 (1985).

[2] L. Landau and E.M. Lifshitz, *Statistical Physics,* Course on Theoretical Physics Vol. 5 (Pergamon Press, Oxford, 1980), 3rd ed., Part 1; S. Alexander and J. McTague, Phys. Rev. Lett. **41**, 702 (1978).

[3] K. Loudiyi and B.J. Ackerson, Physica (Amsterdam) **184A**, 1 (1992).

[4] K. Loudiyi and B.J. Ackerson, Physica (Amsterdam) **184A**, 26 (1992).

[5] H. Xu and M. Baus, Phys. Lett. A **117**, 127 (1986); see also J.L. Barrat and H. Xu, J. Phys. Condens. Matter **2**, 9445 (1990).

[6] J. Chakrabarti, H.R. Krishnamurthy, and A.K. Sood, Phys. Rev. Lett. **73**, 2923 (1994).

[7] For example, see A.K. Sood, in *Solid State Physics,* edited by E. Ehrenreich and D. Turnbull (Academic Press, New York, 1991), Vol. 45, p. 1.

[8] The 3D DLVO potential should also be appropriate for 2D colloids confined between two boundaries with separation $L_z > \kappa^{-1}$. [For example, in Ref. [1], $L_z \simeq 30$ μm, whereas $\kappa^{-1} \simeq 0.3$ μm.]

[9] Murty S.S. Challa, D.P. Landau, and K. Binder, Phys. Rev. B **34**, 1481 (1986); D. Marx, S. Sengupta, O. Opitz, P. Nielaba, and K. Binder, Mol. Phys. **83**, 31 (1994).

[10] M.P. Allen and D.J. Tildesley, *Computer Simulation of Liquids* (Oxford University Press, New York, 1987).

[11] The equilibration time τ_{eq}, which is strongly dependent on L, κa_s, and βV_e, was typically higher for larger L, and was the highest for κa_s values corresponding to a peak in C_V for a given L and βV_e. The crystalline phases typically equilibrated faster than the liquid phases. For a given L and κa_s, τ_{eq} increased with increasing βV_e. Specifically, for a 10×10 lattice, in the (modulated) liquid phase, $\tau_{\text{eq}} \simeq 30\,000$ MC steps for $\beta V_e = 0$ and $\simeq 50\,000$ MC steps for $\beta V_e = \infty$. The increase results from the fact that, as βV_e increases, both V_e and the repulsive interparticle interaction induce partial ordering and restrict particle movements.

[12] However, the value 1.24 for the exponent $(d - \alpha/\nu)$ cannot be regarded as characterizing the real critical behavior, because of finite size effects and insufficient data close enough to the transition.

[13] For $\beta V_e = \infty$ the κa_s values for the transition in ρ_m have an even stronger L dependence, but again extrapolate to the same $\kappa^* a_s$ as obtained using $\kappa_L^* a_s$ (which have a weak L dependence in this case also). These are clearly interesting finite size effects, and need to be studied further.

[14] Loudiyi and Ackerson [4] also noted that for very high external potential the particles become more localized in a direction normal to the potential minima but the order decreases parallel to the minima. This observation can be understood in terms of the reentrant liquid phase in the phase diagram.

[15] An approximate inclusion of fluctuations of the order parameters indeed does yield results consistent with the qualitative features of the simulation phase diagram in the limit of large βV_e. [J. Chakrabarti and Supurna Sinha (unpublished)].